THE JOURNAL OF BIOLOGICAL CHEMISTRY
Vol. 279, No. 45, Issue of November 5, pp. 46907–46914, 2004
Printed in U.S.A.

Reduced β-Amyloid Production and Increased Inflammatory Responses in Presenilin Conditional Knock-out Mice*

Received for publication, August 19, 2004
Published, JBC Papers in Press, September 1, 2004, DOI 10.1074/jbc.M409544200

Vassilios Beglopoulos‡§, Xiaoyan Sun‡§, Carlos A. Saura‡, Cynthia A. Lemere‡, Richard D. Kim¶, and Jie Shen‡‖

From the ‡Center for Neurologic Diseases, Brigham and Women's Hospital, Program in Neuroscience, Harvard Medical School and the ¶Harvard-Partners Center for Genetics and Genomics, Boston, Massachusetts 02115

Mutations in presenilins (PS) 1 and 2 are the major cause of familial Alzheimer's disease. Conditional double knock-out mice lacking both presenilins in the postnatal forebrain (*PS* cDKO mice) exhibit memory and synaptic plasticity impairments followed by progressive neurodegeneration in the cerebral cortex. Here we further investigate the molecular events that may underlie the observed phenotypes and identify additional neuropathological markers in the *PS* cDKO brain. Enzyme-linked immunosorbent assay analysis showed reduced levels of the toxic β-amyloid (Aβ) peptides in the cerebral cortex of *PS* cDKO mice. Interestingly, the reduction in Aβ40 and Aβ42 peptides is similar in *PS1* conditional knock-out and *PS* cDKO mice. We further examined the gene expression profile by oligonucleotide microarrays in the *PS* cDKO cerebral cortex and found that a high number of genes are differentially expressed, most notably a group of up-regulated inflammatory genes. Quantitative real-time reverse transcription PCR and Western analyses confirmed the elevated levels of glial fibrillary acidic protein, complement component C1q, and cathepsin S, up-regulation of which has been associated with inflammatory responses in various neurodegenerative processes. Immunohistochemical analysis revealed that the increase in complement component C1q is confined to the hippocampal formation, whereas glial fibrillary acidic protein and cathepsin S are up-regulated throughout the entire neocortex and hippocampus. In addition, strong microglial activation occurs in the hippocampus and the deeper cortical layers of *PS* cDKO mice. These results indicate that the memory impairment and neurodegeneration in *PS* cDKO mice are not caused by Aβ accumulation and that loss of PS function leads to differential up-regulation of inflammatory markers in the cerebral cortex.

Alzheimer's disease (AD)[1] is the most common form of dementia in the elderly population. Mutations in presenilins 1 and 2 (PS1 and PS2) are the major cause of familial Alzheimer's disease (1). Studies on *PS1*-null mice have revealed essential roles of PS1 in cortical development and γ-secretase cleavage of the amyloid precursor protein (APP) and Notch1 (Ref. 2–6). In contrast to *PS1*-null mice, which are perinatally lethal (2), *PS2*-null mice are viable (7, 8), but mice lacking both presenilins display early embryonic lethality (8, 9). To study PS function in the adult cerebral cortex, which is the most relevant experimental system with respect to AD pathogenesis, we have previously generated presenilin conditional double knock-out (*PS* cDKO) mice lacking both presenilins in excitatory neurons of the forebrain after about postnatal day 18 (10, 11). These mice exhibit memory and synaptic plasticity deficits at the age of 2 months that become more severe as the mouse ages and are accompanied by neuronal degeneration in the cerebral cortex in an age-dependent manner (11). These impairments are associated with reductions in *N*-methyl-D-aspartate receptor-mediated responses and in the expression of CBP and of CREB/CBP downstream genes (11). These findings demonstrate that presenilins have important functions in the adult cerebral cortex.

The purpose of the current study is to investigate further what alterations at the molecular level underlie the impairments caused by presenilin inactivation in the adult brain and to search for additional neuropathological markers in the cerebral cortex of *PS* cDKO mice. Because β-amyloid (Aβ) peptides, which have neurotoxic properties at increased levels, are products of the presenilin-dependent γ-secretase cleavage of APP, we examined Aβ levels in the cerebral cortex of *PS* cDKO mice and found a significant decrease of both Aβ40 and Aβ42. As an approach to search for gene expression changes in the cerebral cortex of *PS* cDKO mice, we performed oligonucleotide microarray analysis and found that a high number of genes are differentially regulated. We further confirmed by quantitative real-time RT-PCR (qRT-PCR) and Western analyses the increase in the levels of a group of genes that are involved in inflammatory responses, and we characterized histologically their up-regulation pattern in the brain of *PS* cDKO mice.

EXPERIMENTAL PROCEDURES

Mice—The generation of *PS1* conditional knock-out (*PS1* cKO), *PS2*−/−, and *PS* cDKO mice has been described previously (7, 10, 11). Neural progenitor cell (NPC)-specific *PS* cDKO mice were generated by crossing floxed *PS1* mice (10), *nestin*-Cre transgenic mice (12), and *PS2*−/− mice (7). The genetic background of all experimental groups used in this study was C57BL6/129 hybrid.

Western Blot—Mouse cerebral cortex was dissected and homogenized in cold buffer (for Fig. 1*A*: 50 mM Tris (pH 7.4), 150 mM NaCl, 2 mM

* This work was supported by a National Institutes of Health Grant NS41783. The costs of publication of this article were defrayed in part by the payment of page charges. This article must therefore be hereby marked "*advertisement*" in accordance with 18 U.S.C. Section 1734 solely to indicate this fact.

§ These authors contributed equally to this work.
‖ To whom correspondence should be addressed: Center for Neurologic Diseases, Harvard New Research Bldg. 636E, 77 Ave. Louis Pasteur, Boston, MA 02115. Tel.: 617-525-5561; Fax: 617-525-5522; E-mail: jshen@rics.bwh.harvard.edu.

[1] The abbreviations used are: AD, Alzheimer's disease; Aβ, β-amyloid; APP, amyloid precursor protein; CREB, cAMP-response element-binding protein; CBP, CREB-binding protein; cDKO, conditional double knock-out; cKO, conditional knock-out; CTF, APP C-terminal fragment; ELISA, enzyme-linked immunosorbent assay; GFAP, glial fibrillary acidic protein; NPC, neuronal progenitor cell; PBS, phosphate-buffered saline; PS, presenilin; qRT-PCR, quantitative real time reverse transcription PCR; RT-PCR, reverse transcription PCR.

EDTA, 1% Nonidet P-40, 0.5% Triton X-100, and protease and phosphatase inhibitors; for Fig. 2*B*: 50 mM Tris (pH 7.4), 150 mM NaCl, 5 mM EDTA, 0.5% Nonidet P-40, 0.5% sodium deoxycholate, 1% SDS, and protease and phosphatase inhibitors). Same amounts of protein were resolved by SDS-PAGE electrophoresis and transferred to polyvinylidene difluoride membranes as described (10). For Fig. 1*A*, blots were incubated with the Saeko antiserum (13) followed by ^{125}I-labeled anti-rabbit antibody (ICN Biomedicals). For Fig. 2*B*, blots were incubated with antibodies against glial fibrillary acidic protein (GFAP) (1:100,000; Sigma), cathepsin S (1:1000; kind gift of Guo-Ping Shi, Boston, MA), or complement component C1q (1:1000; Quidel) and developed with enhanced chemiluminescence (PerkinElmer Life Sciences). For Fig. 2*B*, blots were re-probed with an antibody against α-tubulin (1:100,000; Sigma) as a loading control. Films exposed by blots probed for cathepsin S were subjected to densitometric analysis using NIH Image software, values were normalized to α-tubulin, and significance was tested *post hoc* using one-factor analysis of variance with Scheffe's S test.

Sandwich Aβ Enzyme-linked Immunosorbent Assay (ELISA)—The sandwich Aβ ELISA was developed as described (14). In brief, NUNC Maxisorb immunoassay plates (96-well) were coated with the antibodies 2G3 (anti-Aβ40) or 21F12 (anti-Aβ42) at 0.3 μg/well in PBS overnight at 4 °C. Plates were subsequently blocked with Block ACE (1:4 dilution of original solution; Snow Brand Milk Products) for 2 h at room temperature and washed with PBS-Tween 20 briefly. The samples were loaded in the wells and incubated overnight at 4 °C. After washing with PBS-Tween 20, the plates were incubated in a solution of biotinylated 4G8 for 2 h at 4 °C. The plates were washed with PBS-Tween 20 twice followed by alkaline phosphatase treatment (streptavidin-conjugated alkaline phosphatase, 1:5000 dilution; Amersham Biosciences) for 1.5 h at 4 °C. The signal was amplified by adding 100 μl of AttoPhos and measured with a Fluoroskan (PerkinElmer Life Sciences). The detection limits are 3.125 pg/ml for both Aβ40 and Aβ42. The final values were normalized to the loading amount of wet tissue and analyzed for significance using the Student's *t* test.

Aβ Extraction from Brain Tissue—Tissue was dissected, weighed, and homogenized in Tris-buffered saline (50 mM Tris and 150 mM NaCl, pH 7.4). The homogenates were centrifuged at 100,000 × *g* for 20 min. The resulting pellets were resuspended in 5 M guanidine, 50 mM Tris, pH 8, and incubated at room temperature for 10–30 min. The suspension was then diluted 1:10 with loading buffer (10% Block ACE) and centrifuged at 11,000 × *g* for 10 min. The supernatant was subjected to Aβ detection.

Microarray Analysis—Total RNA was purified from the cerebral cortex of a *PS* cDKO and a control mouse using the TRI reagent (Sigma). RNA was reverse-transcribed, biotin-labeled, and hybridized onto murine MG-U74A GeneChip probe arrays (Affymetrix) following the protocol detailed by Affymetrix. Analysis of differential expression was performed using DNA-Chip Analyzer (dChip) (15). Genes with mean value >60 were analyzed further by cross-comparison between *PS* cDKO and control.

Quantitative Real Time RT-PCR—Quantitative real time RT-PCR was performed as described (11). Briefly, total cortical RNA was treated with DNase I and reverse transcribed in the presence of random hexamers. PCR reactions were performed using SYBR Green PCR Master Mix in an ABI PRISM 7700 Sequence Detector (Applied Biosystems) with 10 μl of diluted (1:25) cDNA and gene-specific primers. Reactions were performed in duplicate, and threshold cycle values were normalized to 18 S RNA. All procedures were carried out together for *PS* cDKO and control in gender-matched pairs. The PCR products were analyzed by electrophoresis to confirm their correct sizes. Significance was tested *post hoc* using one-factor analysis of variance with a Scheffe's S test.

Immunohistochemistry—For cathepsin S, complement component C1q, and CD45 immunostainings, mice were sacrificed with CO_2 and transcardially perfused with PBS followed by 4% paraformaldehyde. Brains were dissected, post-fixed for 2 h at room temperature, and cryoprotected in 30% sucrose for 48 h at 4 °C. Cryostat sagittal sections were cut (10 μm for cathepsin S and 30 μm for complement component C1q and CD45 immunostaining) and incubated with antibodies against cathepsin S (1:30, Santa Cruz Biotechnology), complement component C1q (1:100, HyCult Biotechnology), or CD45 (1:1000, Serotec). For GFAP immunostaining, mice were sacrificed with CO_2 and perfused with PBS, brains were fixed in 10% formalin for 2 h at room temperature and paraffin-embedded, and 10-μm sagittal sections were cut and incubated with an antibody against GFAP (1:500; Sigma). For all immunostaining, detection was performed using an avidin-biotin complex (ABC) kit (Vectastain) and a 3,3-diaminobenzimide (DAB) substrate kit for peroxidase (Vector Laboratories) without Ni^{2+} (brown color) for GFAP and C1q detection or with Ni^{2+} (black color) for cathepsin S and CD45 detection. Images were captured using an Olympus BX40 light microscope.

RESULTS

To evaluate the potential involvement of altered APP processing in the phenotypes observed in *PS* cDKO mice, we examined APP processing in the cerebral cortex of *PS* cDKO mice. The substrates for γ-secretase-mediated proteolysis of APP are the APP C-terminal fragments (CTFs), which are products of α- and β-secretase activities and accumulate in the absence of γ-secretase cleavage. To determine the levels of CTFs in the cerebral cortex of *PS* cDKO mice, we performed Western analysis using an antiserum (Saeko) that detects the C-terminal region of APP (13). At 2 and 6 months of age we observed accumulation of CTFs in *PS* cDKO mice in comparison with control and *PS2*−/− mice (Fig. 1*A*). The degree of accumulation was slightly higher than that seen in *PS1* cKO mice, with similar patterns at 2 and at 6 months of age (Fig. 1*A*).

Next, we used an ELISA to determine the levels of Aβ peptides in the cerebral cortex of *PS* cDKO mice. We first measured generation of Aβ40 and Aβ42 peptides in the cerebral cortex of 6-month-old mice and found a significant reduction of both species in *PS* cDKO as compared with control and *PS2*−/− mice (Fig. 1*B*). Interestingly, similar reductions were found in *PS* cDKO and *PS1* cKO mice (Fig. 1*B*). Given the difference in the severity of the phenotypes between 2-month-old and 6-month-old *PS* cDKO mice (11), we next asked whether the degree of reduction in Aβ levels is also different between these two time points. ELISA measurements at the age of 2 months also showed a significant decrease of Aβ40 and Aβ42 in the *PS* cDKO cerebral cortex, as compared with control, at similar levels as the decrease observed at 6 months (Fig. 1*C*). These results demonstrate that the reduction in the presenilin-mediated γ-secretase cleavage of APP in *PS* cDKO mice is similar to that in *PS1* cKO mice and is age-independent.

Because a small amount of Aβ was still detected in the cortex of *PS* cDKO mice, which could be due to expression of PS1 in glial cells and/or interneurons, we measured Aβ levels in another line of nervous system-specific *PS* cDKO mice (NPC-*PS* cDKO mice) in which Cre recombinase is expressed under the control of the *nestin* promoter (12); thus, *PS1* expression is inactivated in neural progenitor cells and NPC-derived neurons and glia. We found that Aβ40 peptides could no longer be detected in whole brain extracts from NPC-*PS* cDKO embryos at day 15.5 (Fig. 1*D*). However, a small amount of Aβ42 was still detected (Fig. 1*D*), suggesting that its production may not be entirely regulated by presenilins.

We next aimed to determine what changes in gene expression are potentially associated with the progressive development of neuropathology in *PS* cDKO mice. We performed oligonucleotide microarray analysis using RNA from the cerebral cortex of 6-month-old mice as an approach to search for differentially expressed genes in large scale. At 6 months of age, *PS* cDKO mice have lost 18% of their cortical neurons and display very severe impairments of learning and memory and synaptic plasticity (11). The gene expression profiles of a *PS* cDKO and a control mouse were compared using oligonucleotide microarrays representing ~12,500 murine characterized genes and expressed sequence tags. Analysis of differential expression was performed using DNA-Chip Analyzer (dChip), a model-based approach computing expression levels for oligonucleotide arrays (15). This algorithm assigns proper weight to each probe within the set of 16 probes that interrogate each gene and influences the calculation of the fold change. 37 characterized genes and expressed sequence tags were found to be >2-fold up-regulated in *PS* cDKO mice (Table I). Classification showed that ~25% of these genes are involved in inflammatory or

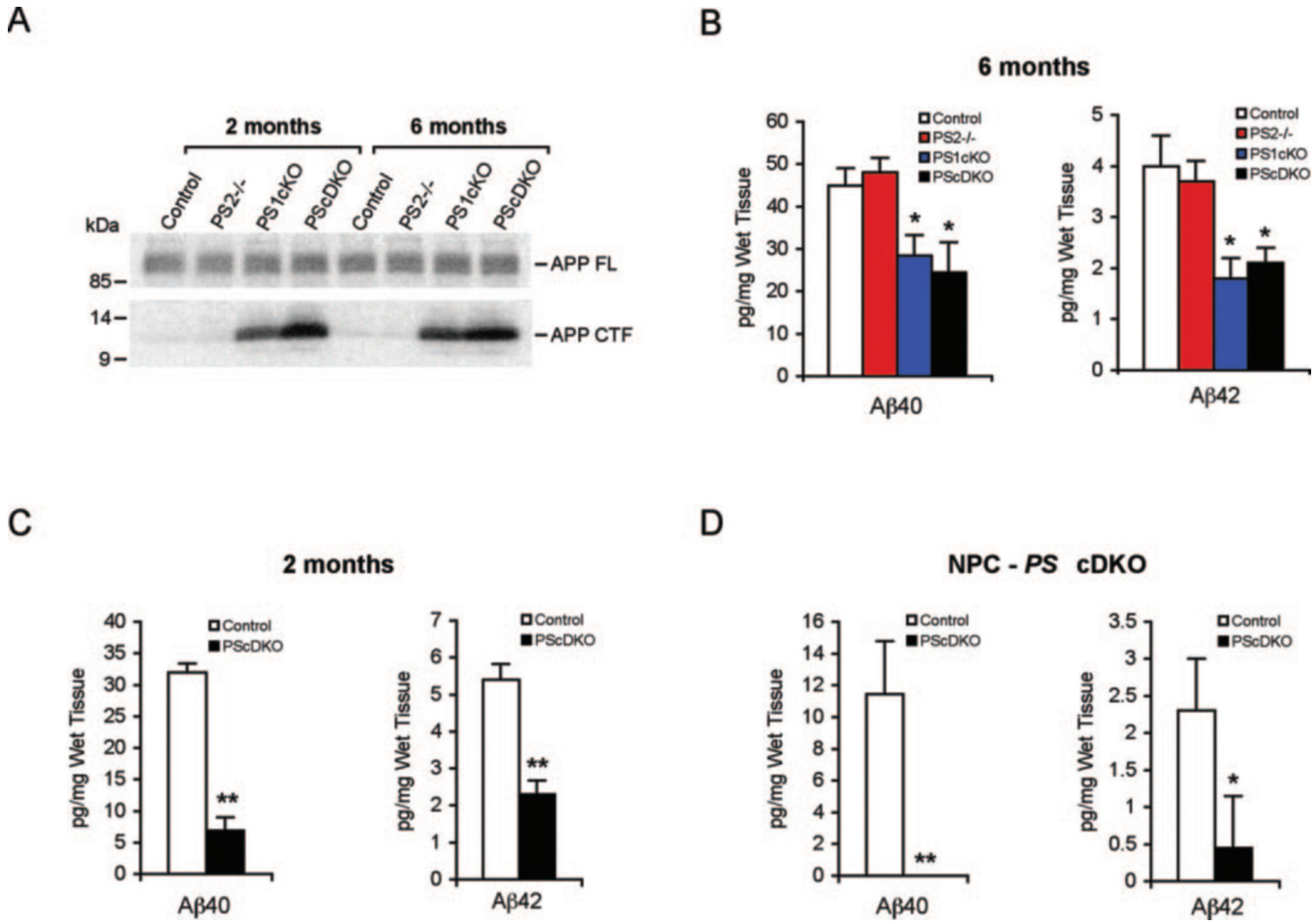

FIG. 1. **Accumulation of CTFs and reduced Aβ production in *PS* cDKO mice.** *A*, Western blot analysis shows accumulation of CTFs in the cerebral cortex of *PS1* cKO and *PS* cDKO mice at 2 and at 6 months of age compared to control and *PS2*−/− mice. *APP FL*, APP full-length. *B*, levels of Aβ40 (*left*) and Aβ42 (*right*) in the cerebral cortex of control ($n = 3$), *PS2*−/− ($n = 3$), *PS1* cKO ($n = 3$), and with *PS* cDKO ($n = 3$) mice at the age of 6 months as measured by ELISA. *Asterisks* represent significance comparisons with control and with *PS2*−/−. *C*, ELISA measurements of Aβ40 (*left*) and Aβ42 (*right*) in the cerebral cortex of control ($n = 3$) and *PS* cDKO ($n = 3$) mice at the age of 2 months. *D*, levels of Aβ40 (*left*) and Aβ42 (*right*) in whole brain extracts from control ($n = 4$) and NPC-*PS* cDKO ($n = 4$) embryos at embryonic day 15.5. *, $p < 0.05$; **, $p < 0.01$.

immune responses, such as GFAP, chains of complement component C1q, and members of the cathepsin family. Ion and gap junction channels, transport/cytoskeleton-related genes, and genes involved in oxidation, signal transduction, or transcription were also among the genes that showed increased levels of expression. There were 26 characterized genes and expressed sequenced tags that were >2-fold down-regulated in *PS* cDKO mice (Table II). As in the case of the up-regulated genes, functional groups included ion channels, transport/cytoskeleton-related genes, and genes involved in transcription. In addition, genes involved in cell growth or metabolism were also decreased.[2]

PS cDKO mice exhibit several morphological hallmarks of synaptic and neuronal loss (11). Based on the *PS* cDKO gene expression profile as revealed by microarray analysis, we investigated further what additional molecular alterations that have been associated with neurodegenerative processes are present in the cerebral cortex of *PS* cDKO mice. GFAP, an intermediate filament protein, is abundantly expressed during astrocytic activation and is present at increased levels in the brain of AD patients (16, 17). As shown in Table I, *GFAP* was found to be one of the most highly up-regulated genes in the cerebral cortex of *PS* cDKO mice by oligonucleotide microarrays. We performed qRT-PCR analysis using RNA from the cerebral cortex of seven *PS* cDKO and seven control mice to further test the levels of GFAP expression with an independent technique. GFAP was found to be ~10-fold elevated in the *PS* cDKO cerebral cortex ($p < 0.0005$; Fig. 2*A*), confirming the microarray result and demonstrating strong astrocytic activation. Western analysis using total cerebral cortical lysates showed a strong GFAP signal in the *PS* cDKO samples, whereas the band in the control samples was out of detection with the antibody dilution used, further verifying the microarray and qRT-PCR results at the protein level (Fig. 2*B*).

Of the inflammation-related genes that were shown higher than 2-fold up-regulated in *PS* cDKO mice (Table I), three genes (complement component C1q α and β polypeptides and complement component 3a receptor 1) are involved in complement system activation. The γ polypeptide of complement component C1q was also found up-regulated by 1.6-fold (data not shown). The complement system is an important part of the immune system, and its activation has been associated with AD pathology and cognitive dysfunction (18). qRT-PCR analysis for the α polypeptide of complement component C1q further showed increased mRNA levels in the cerebral cortex of *PS* cDKO mice by ~4-fold ($p < 0.00001$; Fig. 2*A*). By Western blot

[2] The *PS* cDKO and control lists of hybridization values for all genes included in the microarrays can be accessed through the Gene Expression Omnibus (GEO) web site at www.ncbi.nlm.nih.gov/geo under accession number GSE1375.

TABLE I
Up-regulated genes in the cerebral cortex of PS cDKO mice

Classification	Gene description	Fold change	GenBank™ accession no.[a]
Inflammation/immune responses	Glial fibrillary acidic protein	6.0	NM_010277
	Killer cell lectin-like receptor, subfamily A, member 3	3.3	NM_010648
	CD9	3.2	NM_007657
	Complement component C1q, β polypeptide	3.0	NM_009777
	Cathepsin C	2.4	NM_009982
	Ia-associated invariant chain	2.1	NM_010545
	Complement component 3a receptor 1	2.1	NM_009779
	Complement component C1q, α polypeptide	2.1	NM_007572
	Cathepsin Z	2.0	NM_022325
Ion/gap junction channels	Na^+ channel, voltage-gated, type X, α polypeptide	2.2	NM_009134
	Gap junction membrane channel protein α1	2.1	NM_010288
Oxidation	Glutathione peroxidase 5	2.6	NM_010343
	Cytochrome c oxidase, subunit VIIIa	2.0	NM_007750
Signal transduction	Guanine nucleotide binding protein, β1	6.9	NM_008142
Transcription	Metal response element binding transcription factor 1	3.1	NM_008636
	Sp100	2.3	NM_013673
	LIM homeobox protein 8	2.1	NM_010713
	Heart and neural crest derivatives expressed transcript 1	2.1	NM_008213
Transport/cytoskeleton	Protein regulator of cytokinesis 1	3.2	NM_145150
	Kinesin family member 5B	3.0	NM_008448
	ATP-binding cassette, sub-family C (CFTR/MRP), member 6	2.8	NM_018795
	Adenylyl cyclase-associated protein 1	2.2	NM_007598
	Solute carrier family 38, member 2	2.0	NM_175121
Miscellaneous	Stabilin 1	2.6	NM_138672
	RIKEN cDNA 2700097O09 gene	2.5	NM_028314
	Murine retrovirus readthrough RNA sequence	2.5	AF014454
	Tyrosinase-related protein 1	2.3	NM_031202
	Tenascin XB	2.1	NM_031176
	Imprinted and ancient (Impact)	2.0	NM_008378
	Signaling molecule ATTP	2.0	NM_016855
	Glucosidase β2	2.0	NM_172692
Expressed sequence tags	EST[b]	3.1	AA536968
	EST[b]	2.5	AA725931
	EST[b]	2.1	AW122725
	EST[b]	2.1	AV138114
	EST[b]	2.1	AV361852
	EST[b]	2.0	AI639614

[a] The RefSeq transcript identifier is given, wherever available.
[b] Expressed sequence tag.

using an antibody against C1q, we observed a strong increase in the *PS* cDKO lysates in the intensity of a band with a molecular mass of 33 kDa corresponding to C1q α and β polypeptides, whereas a very faint band was observed in the control lysates (Fig. 2*B*). The C1q γ polypeptide, with molecular mass of 24 kDa, was under detection in both *PS* cDKO and control lysates.

Members of the cathepsin protease family (cathepsins C and Z) were also among the genes that were found at increased levels in *PS* cDKO mice (Table I). Another member of the same family, cathepsin S, was shown 1.8-fold increased (data not shown). Cathepsin S is a lysosomal cysteine protease and is elevated in the brain of AD and Down syndrome patients (19). qRT-PCR analysis further showed up-regulation of cathepsin S in the cerebral cortex of *PS* cDKO mice (~2.6-fold, $p < 0.005$; Fig. 2*A*). By Western blot, cathepsin S was also found at higher levels in the *PS* cDKO compared with control lysates (Fig. 2*B*). Densitometric analysis of the cathepsin S bands from lysates from nine *PS* cDKO and seven control mice, after normalization to α-tubulin as a loading control, showed a significant increase in band intensity in the *PS* cDKO lysates (~2.1-fold, $p < 0.03$).

We next addressed the localization of the up-regulated proteins in the brain of *PS* cDKO mice by means of immunohistochemistry. Increased GFAP immunoreactivity, indicative of astrogliosis, was seen throughout the neocortex and hippocampus of *PS* cDKO mice, strongly labeling astrocytes with the typical morphology of their activated state (Fig. 3). Immunohistochemistry using an antibody against cathepsin S showed a dramatic elevation of cathepsin S-positive cells in *PS* cDKO mice compared with control mice, where immunoreactivity was virtually absent (Fig. 3). Staining was observed throughout the neocortex (Fig. 3*A*) as well as in the stratum oriens and stratum radiatum of the hippocampus proper (Fig. 3*B*), the lacunosum moleculare layer, and the dentate gyrus molecular layer (data not shown). Up-regulated cathepsin S was found in a punctate pattern, reflecting its lysosomal distribution. By double labeling for cathepsin S and GFAP we observed no colocalization (data not shown), suggesting that the cells bearing increased levels of cathepsin S in *PS* cDKO mice may not be astrocytes.

Interestingly, immunostaining for complement component C1q revealed no immunoreactivity in the neocortex (Fig. 3*A*) but a marked increase in immunoreactivity in the *PS* cDKO hippocampus compared with the control (Fig. 3*B*). Staining in *PS* cDKO mice was observed in a diffuse pattern and was present in the stratum oriens, stratum radiatum, and molecular layers of the hippocampus (Fig. 3*B* and data not shown). In control mice, staining was clearly observed only in the molecular layers of the hippocampus at levels similar to or lower than those in *PS* cDKO mice (data not shown) and was very weak or absent in the stratum oriens and stratum radiatum (Fig. 3*B*).

Given the high inflammatory responses observed in *PS* cDKO mice, we next addressed whether microglial activation,

TABLE II
Down-regulated genes in the cerebral cortex of PS cDKO mice

Classification	Gene description	Fold change	GenBank™ accession no.[a]
Cell growth	Thyroid stimulating hormone, β-subunit	−2.8	NM_009432
	Growth arrest specific 5	−2.3	NM_013525
	Epithelial membrane protein 1	−2.2	NM_010128
	Growth/differentiation factor 11	−2.1	AF100906
Ion channels/receptors	K^+ voltage-gated channel, shaker-related subfamily, β2	−4.6	NM_010598
	Coagulation factor II (thrombin) receptor	−2.4	NM_010169
	K^+ voltage-gated channel, Isk-related subfamily, member 1	−2.3	NM_008424
	Frizzled-4	−2.1	NM_008055
Metabolism	Hydroxysteroid (17-β) dehydrogenase 1	−2.7	NM_010475
	Dehydrogenase/reductase (SDR family) member 7	−2.1	NM_025522
	Fatty acid coenzyme A ligase, long chain 2	−2.0	NM_007981
Transcription	D site albumin promoter-binding protein	−2.5	NM_016974
	Forkhead box O3	−2.3	NM_019740
	Small nuclear RNA activating complex, polypeptide 3	−2.3	NM_029949
	Caudal type homeobox 1	−2.0	NM_009880
Transport/cytoskeleton	Proline-serine-threonine phosphatase-interacting protein 1	−2.2	NM_011193
	Rho GDP dissociation inhibitor (GDI) γ	−2.1	NM_008113
Miscellaneous	Cytohesin-binding protein	−3.3	NM_139200
	Zinc finger protein 101	−2.8	NM_009542
	Histocompatibility 2, T region locus 23	−2.7	Y00629
	Similar to KIAA0561 protein	−2.2	NM_199308
	Ectonucleotide pyrophosphatase/phosphodiesterase 2	−2.1	NM_015744
	Erythroid differentiation regulator	−2.0	AJ007909
Expressed sequence tags	EST[b]	−2.5	AI153421
	EST[b]	−2.3	AI536457
	EST[b]	−2.1	AI845165

[a] The RefSeq transcript identifier is given, wherever available.
[b] Expressed sequence tag.

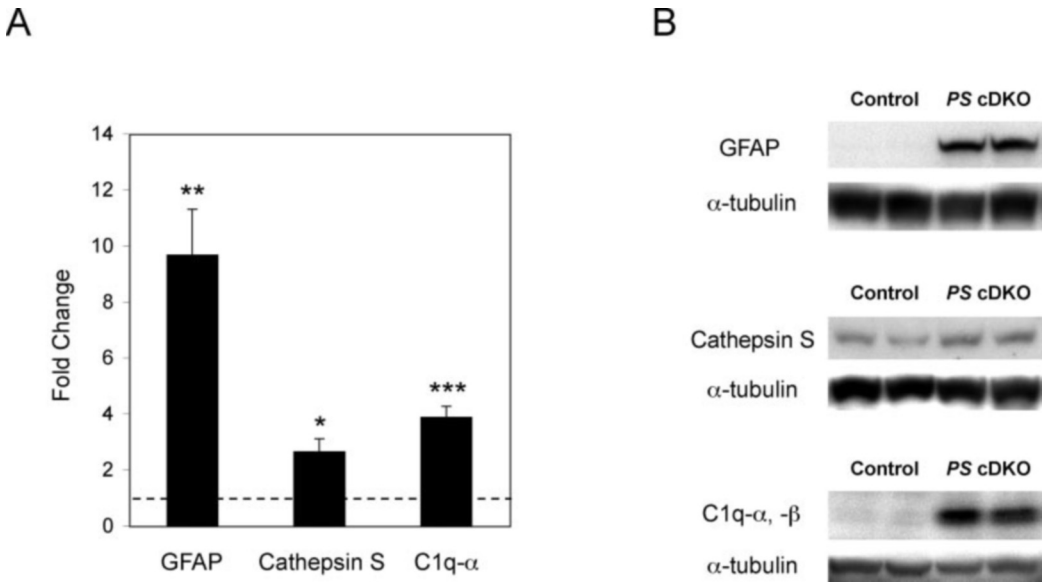

FIG. 2. **Increased mRNA and protein levels of GFAP, cathepsin S, and complement component C1q in *PS* cDKO mice.** *A*, quantitative real time RT-PCR analysis using RNA from the cerebral cortex of seven *PS* cDKO mice and seven control mice at 6 months of age confirms the up-regulation at the mRNA levels of GFAP, cathepsin S, and complement component C1q α polypeptide. The *dotted line* indicates control levels. *, $p < 0.005$; **, $p < 0.0005$; ***, $p < 0.00001$. *B*, Western blot analysis shows increased protein levels of GFAP, cathepsin S, and the α and β polypeptides of complement component C1q in the cerebral cortex of 6-month-old *PS* cDKO mice as compared with control mice. Membranes were re-probed with an antibody against α-tubulin as a loading control. Molecular masses: GFAP, 50–55 kDa; cathepsin S, 28 kDa; C1q-α and -β polypeptides, 33 kDa; α-tubulin, 55–60 kDa.

another important inflammatory mechanism, is also present in the *PS* cDKO brain. By immunostaining using an antibody against CD45, a transmembrane glycoprotein widely used as a microglial marker, we observed a strong increase in immunoreactivity in the hippocampus of *PS* cDKO compared with control mice, with a cellular staining pattern typical of the morphology of activated microglia (Fig. 3*B*). Staining was also observed at increased levels in the neocortex, mainly at the deeper layers (Fig. 3*A*). Labeled activated microglia in the hippocampus of *PS* cDKO mice were present in the stratum oriens and stratum radiatum (Fig. 3*B*), the lacunosum moleculare layer, and the dentate gyrus molecular and polymorph layers (data not shown).

DISCUSSION

We have shown previously that inactivation of presenilins in the adult cerebral cortex results in impairments of learning and memory, synaptic plasticity, and neuronal survival in an

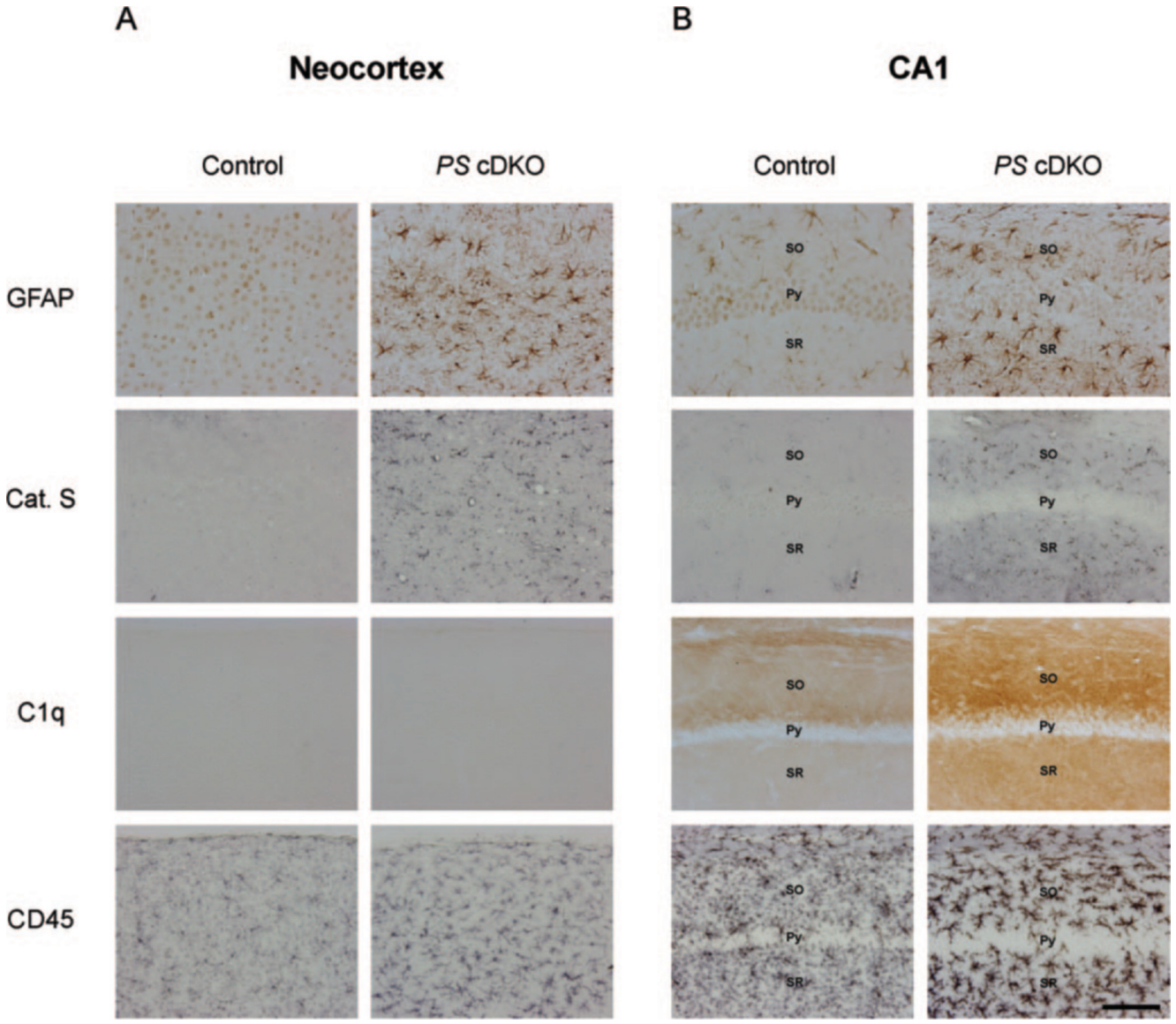

FIG. 3. **Inflammatory responses in the neocortex and hippocampus of *PS* cDKO mice.** Immunohistochemistry for GFAP, cathepsin S, complement component C1q, and CD45 on sagittal brain sections from control and *PS* cDKO mice at 6–7 months of age reveals high increases in immunoreactivity in the *PS* cDKO brain. Light microscope pictures of the neocortex are shown in *panel A* and of the CA1 region of the hippocampus in *panel B*. Staining for GFAP labels activated astrocytes throughout the neocortex and hippocampus of *PS* cDKO mice, whereas in the control sections only background staining is present in the neocortex and a few labeled astrocytes are present in the hippocampus. High cathepsin S immunoreactivity is observed in both the neocortex and hippocampus of *PS* cDKO mice, whereas virtually no staining is seen in the control sections. Cathepsin S is present in a punctate pattern, reflecting its lysosomal distribution. Complement component C1q is up-regulated only in the hippocampus of *PS* cDKO mice, whereas no staining is observed in the neocortex. For both cathepsin S and complement component C1q, immunoreactivity in the *PS* cDKO hippocampus is defined in the stratum oriens and stratum radiatum of the hippocampus proper, as shown for the CA1 region in *panel B*, as well as in the lacunosum moleculare layer and the dentate gyrus molecular layer. Strongly activated microglia labeled with CD45 are present in the hippocampus of *PS* cDKO mice as well as in the neocortex, mainly at the lower layers. *SO*, stratum oriens; *Py*, pyramidal cell layer; *SR*, stratum radiatum. *Scale bar*, 100 μm.

age-dependent manner (11). *PS* cDKO mice also exhibit reductions in *N*-methyl-D-aspartate receptor-mediated responses and in the expression of CBP and of CREB/CBP downstream genes (11). The striking neuropathological phenotypes of *PS* cDKO mice prompted us to investigate further the molecular events that underlie the observed phenotypes.

A well established role of presenilins is the control of APP processing via their function as components of the γ-secretase complex that generates Aβ from APP CTFs. Aβ peptides and particularly Aβ42 are known to have neurotoxic properties at increased levels, which could be relevant to the deficits observed in *PS* cDKO mice. Our data, however, argue against this idea because the levels of Aβ40 and Aβ42 are significantly reduced in the *PS* cDKO cerebral cortex. The degree of reduction was found to be similar to that in *PS1* cKO mice, confirming that PS1 is responsible for the majority of Aβ production *in vivo*. The small amount of residual Aβ likely reflects the presence of PS1 in glial cells and interneurons lacking Cre expression. To verify this hypothesis, we further examined the levels of Aβ40 and Aβ42 in NPC-*PS* cDKO mice, which lack presenilins in all cells in the nervous system. Aβ40 was under the detection limits of the assay, confirming that its generation is totally controlled by presenilins. Interestingly, we could still detect Aβ42, raising the possibility that additional enzymatic activities other than presenilin-controlled γ-secretase may also be responsible for production of Aβ42, as has been suggested previously by studies in cultured cells (20, 21). Although the phenotypes in *PS* cDKO mice could theoretically be caused by

the reduction in Aβ peptides, this is unlikely for the following reasons. First, the levels of Aβ40 and Aβ42 are reduced to similar extents in *PS* cDKO and *PS1* cKO mice despite the severe impairments in the former and the absence of neurodegeneration and synaptic plasticity deficits in the latter (10, 11). Second, *PS* cDKO mice exhibit much more severe phenotypes than *APP*-null mice, in which Aβ peptides are absent (22). Our results therefore indicate that the neuropathology in *PS* cDKO mice is independent of Aβ generation.

Despite the similar Aβ levels in *PS* cDKO and *PS1* cKO mice, the amount of CTFs was slightly higher in the *PS* cDKO cerebral cortex. The absence of correlation between reduced Aβ production and CTF accumulation has been reported previously in cultured cells expressing mutant forms of PS1, suggesting roles of PS1 in CTF degradation or APP trafficking (23–25). Our results suggest that, in the adult brain, PS2 has a more evident function in potential direct effects on CTF production and/or degradation than in the control of Aβ generation. CTF expression in transgenic mice results in impaired learning, long-term potentiation, and neuronal survival (26, 27), which could lead to the idea that the increase in CTF levels may contribute to the *PS* cDKO pathology. The deficits in CTF-expressing transgenic mice, though, are associated with increased Aβ immunoreactivity (27, 28), therefore rendering unclear whether CTF alone is responsible for the phenotypes observed. Injection of recombinant CTFs into mice has been reported to have neurotoxic properties (29), raising the possibility of harmful effects of the increased CTFs in *PS* cDKO mice. However, it is unknown whether the respective native fragment could exert the same effect in increased levels. Also, the concentration of recombinant CTFs in the brain after injection is likely to be much higher than the difference in CTF concentration between *PS* cDKO and *PS1* cKO mice. Because *PS1* cKO mice exhibit only a very mild phenotype (10) but display comparable CTF levels with *PS* cDKO mice, it is unlikely that the small increase in CTF production could account for the observed impairments.

Gene expression profile studies are becoming increasingly valuable as an approach to delineate alterations at the molecular level that are associated with genetic manipulations and to attribute specific phenotypes to groups of functionally related genes. Here we show, by oligonucleotide microarray analysis, that differential expression of distinct groups of genes accompanies the pathology in *PS* cDKO mice. Most notably, genes that are involved in inflammatory responses are up-regulated in the *PS* cDKO cerebral cortex. We further confirmed by qRT-PCR, Western blot, and immunohistochemical analyses that the levels of GFAP are elevated in the cerebral cortex of *PS* cDKO mice. Increased expression of GFAP has been suggested to be among the earliest and most sensitive features of neuronal toxicity (30). Reactive astrocytes, of which GFAP is a marker, are present in Aβ plaques in the brain of AD patients (31–33). However, it has been reported that astrogliosis in the AD brain, as measured by GFAP levels, increases independently of Aβ accumulation but correlates with the duration of the disease, suggesting that it is not a response to Aβ but likely a reaction to neuronal and synaptic loss and tangle formation (17). *PS* cDKO mice exhibit reduced levels of Aβ in the cerebral cortex (Fig. 1) but develop synaptic loss and progressive neurodegeneration (11). Therefore, our finding that GFAP is up-regulated in *PS* cDKO mice is consistent with the idea that synaptic and neuronal loss can result in astrogliosis independently of Aβ.

The complement system, a significant part of the immune system used to target toxic substances, is involved in inflammatory responses in the brain of AD and Down syndrome patients (18). We show by a variety of different techniques that the initial part of the classical complement pathway, complement component C1q, is increased in *PS* cDKO mice. Interestingly, complement activation in *PS* cDKO mice occurs only in the hippocampus, with complete absence in the neocortex. This pattern presents the first morphological phenotype caused by loss of PS function *in vivo* that is clearly distinct between the neocortex and the hippocampus, although PS inactivation occurs to the same extent and under a similar time course in both regions (10, 11). The functional significance of this disparity and its possible correlation with other phenotypes constitute interesting subjects of potential future studies. C1q immunoreactivity in *PS* cDKO mice appears in a diffuse pattern likely representing localization at the neuropil, which at the age of the mice used for the analysis (6 months) is in the process of degeneration, as indicated by reduced dendritic and synaptic density (11). The characteristics of C1q staining in *PS* cDKO mice are in strong contrast with the pattern reported in transgenic mice carrying pathogenic mutations of APP and PS1, in which C1q is colocalized with fibrillar Aβ plaques and plaque-associated microglia (34). This difference could be expected based on the absence of amyloid plaques in *PS* cDKO mice, and it is interesting that two mouse lines with different PS mutations both exhibit activation of the complement system, but in highly divergent patterns.

Our results show that cathepsin S, a lysosomal cysteine protease important for normal major histocompatibility class II-dependent immunity (35), is up-regulated in the neocortex and the hippocampus of *PS* cDKO mice. Cathepsin S is secreted from microglia and macrophages in response to stimulation with inflammatory mediators, and its expression is strongly elevated after entorhinal cortex lesion of adult rat brain (36). Interestingly, cathepsin S immunoreactivity has been found to be increased in the brain of AD and Down syndrome patients (19). A more thorough comparison between the mechanisms that lead to cathepsin S up-regulation in *PS* cDKO mice and those that lead to its up-regulation in human disease or other animal models remains to be addressed in the future.

Activated microglia are mediators of inflammatory responses in several neuropathological conditions and are important targets for research in AD inflammation (31). Our immunohistochemical analysis using the microglial marker CD45 showed that strong microglial activation occurs in the brain of *PS* cDKO mice, most prominently in the hippocampal formation. When activated, microglia are capable of producing a variety of inflammatory molecules such as cytokines and reactive oxygen intermediates (31). Given the widespread inflammatory reaction observed in the brain of *PS* cDKO mice, as evidenced by strong astrocytic and microglial activations and increased levels of complement component C1q and cathepsin S, it is likely that a vast array of additional molecular mediators of inflammation are also present at high levels in the *PS* cDKO brain.

In summary, our results investigate how APP processing is affected by loss of presenilin function in the adult brain and characterize at the molecular, biochemical, and morphological level several inflammatory responses in the cerebral cortex of *PS* cDKO mice. These findings identify additional molecular events that underlie the observed phenotypes and provide further evidence that *PS* cDKO mice are a valuable model system of neuropathology associated with progressive neurodegeneration.

Acknowledgments—We thank G.-P. Shi for cathepsin S antibody (used for Western blot) and W. Cheng, D. Kim, and S. Malkani for assistance.

REFERENCES

1. Hutton, M., and Hardy, J. (1997) *Hum. Mol. Genet.* **6,** 1639–1646
2. Shen, J., Bronson, R. T., Chen, D. F., Xia, W., Selkoe, D. J., and Tonegawa, S. (1997) *Cell* **89,** 629–639
3. De Strooper, B., Saftig, P., Craessaerts, K., Vanderstichele, H., Guhde, G., Annaert, W., Von Figura, K., and Van Leuven, F. (1998) *Nature* **391,** 387–390
4. De Strooper, B., Annaert, W., Cupers, P., Saftig, P., Craessaerts, K., Mumm, J. S., Schroeter, E. H., Schrijvers, V., Wolfe, M. S., Ray, W. J., Goate, A., and Kopan, R. (1999) *Nature* **398,** 518–522
5. Song, W., Nadeau, P., Yuan, M., Yang, X., Shen, J., and Yankner, B. A. (1999) *Proc. Natl. Acad. Sci. U. S. A.* **96,** 6959–6963
6. Handler, M., Yang, X., and Shen, J. (2000) *Development* **127,** 2593–2606
7. Steiner, H., Duff, K., Capell, A., Romig, H., Grim, M. G., Lincoln, S., Hardy, J., Yu, X., Picciano, M., Fechteler, K., Citron, M., Kopan, R., Pesold, B., Keck, S., Baader, M., Tomita, T., Iwatsubo, T., Baumeister, R., and Haass, C. (1999) *J. Biol. Chem.* **274,** 28669–28673
8. Herreman, A., Hartmann, D., Annaert, W., Saftig, P., Craessaerts, K., Serneels, L., Umans, L., Schrijvers, V., Checler, F., Vanderstichele, H., Baekelandt, V., Dressel, R., Cupers, P., Huylebroeck, D., Zwijsen, A., Van Leuven, F., and De Strooper, B. (1999) *Proc. Natl. Acad. Sci. U. S. A.* **96,** 11872–11877
9. Donoviel, D. B., Hadjantonakis, A., Ikeda, M., Zheng, H., St George Hyslop, P., and Bernstein, A. (1999) *Genes Dev.* **13,** 2801–2810
10. Yu, H., Saura, C. A., Choi, S.-Y., Sun, L. D., Yang, X., Handler, M., Kawarabayashi, T., Younkin, L., Fedeles, B., Wilson, M. A., Younkin, S., Kandel, E. R., Kirkwood, A., and Shen, J. (2001) *Neuron* **31,** 713–726
11. Saura, C. A., Choi, S.-Y., Beglopoulos, V., Malkani, S., Zhang, D., Rao, B. S. S., Chattarji, S., Kelleher, R. J., III, Kandel, E. R., Duff, K., Kirkwood, A., and Shen, J. (2004) *Neuron* **42,** 23–36
12. Tronche, F., Kellendonk, C., Kretz, O., Gass, P., Anlag, K., Orban, P. C., Bock, R., Klein, R., and Schutz, G. (1999) *Nat. Genet.* **23,** 99–103
13. Kawarabayashi, T., Shoji, M., Sato, M., Sasaki, A., Ho, L., Eckman, C. B., Prada, C. M., Younkin, S. G., Kobayashi, T., Tada, N., Matsubara, E., Iizuka, T., Harigaya, Y., Kasai, K., and Hirai, S. (1996) *Neurobiol. Aging* **17,** 215–222
14. Sun, X., Sato, S., Murayama, O., Murayama, M., Park, J. M., Yamaguchi, H., and Takashima, A. (2002) *Neurosci. Lett.* **321,** 61–64
15. Li, C., and Wong, W. H. (2001) *Proc. Natl. Acad. Sci. U. S. A.* **98,** 31–36
16. Overmyer, M., Helisalmi, S., Soininen, H., Laakso, M., Riekkinen, P. S., and Alafuzoff, I. (1999) *Dement. Geriatr. Cogn. Disord.* **10,** 252–257
17. Ingelsson, M., Fukumoto, H., Newell, K. L., Growdon, J. H., Hedley-Whyte, E. T., Frosch, M. P., Albert, M. S., Hyman, B. T., and Irizarry, M. C. (2004) *Neurology* **62,** 925–931
18. Tenner, A. J. (2001) *Neurobiol. Aging* **22,** 849–861
19. Lemere, C. A., Munger, J. S., Shi, G.-P., Natkin, L., Haass, C., Chapman, H. A., and Selkoe, D. J. (1995) *Am. J. Pathol.* **146,** 848–860
20. Armogida, M., Petit, A., Vincent, B., Scarzello, S., da Costa, C. A., and Checler, F. (2001) *Nat. Cell Biol.* **3,** 1030–1033
21. Wilson, C. A., Doms, R. W., Zheng, H., and Lee, V. M. (2002) *Nat. Neurosci.* **5,** 849–855
22. Zheng, H., Jiang, M. H., Trumbauer, M. E., Sirinathsinghji, D. J. S., Hopkins, R., Smith, D. W., Heavens, R. P., Dawson, G. R., Boyce, S., Conner, M. W., Stevens, K., Slunt, H. H., Sisodia, S. S., Chen, H. Y., and Van der Ploeg, L. H. T. (1995) *Cell* **81,** 525–531
23. Capell, A., Steiner, H., Romig, H., Keck, S., Baader, M., Grim, M. G., Baumeister, R., and Haass, C. (2000) *Nat. Cell Biol.* **2,** 205–211
24. Kim, S.-H., Leem, J. Y., Lah, J. J., Slunt, H. H., Levey, A. I., Thinakaran, G, and Sisodia, S. S. (2001) *J. Biol. Chem.* **276,** 43343–43350
25. Leem, J. Y., Saura, C. A., Pietrzik, C., Christianson, J., Wanamaker, C., King, L. T., Veselits, M. L., Tomita, T., Gasparini, L., Iwatsubo, T., Xu, H., Green, W. N., Koo, E. H., and Thinakaran, G. (2002) *Neurobiol. Dis.* **11,** 64–82
26. Oster-Granite, M. L., McPhie, D. L., Greenan, J., and Neve, R. L. (1996) *J. Neurosci.* **16,** 6732–6741
27. Nalbantoglu, J., Tirado-Santiago, G., Lahsaini, A., Poirier, J., Goncalves, O., Verge, G., Momoli, F., Welner, S. A., Massicotte, G., Julien, J. P., and Shapiro, M. L. (1997) *Nature* **387,** 500–505
28. Kammesheidt, A., Boyce, F. M., Spanoyannis, A. F., Cummings, B. J., Ortegon, M., Cotman, C., Vaught, J. L., and Neve, R. L. (1992) *Proc. Natl. Acad. Sci. U. S. A.* **89,** 10857–10861
29. Song, D.-K., Won, M.-H., Jung, J.-S., Lee, J.-C., Kang, T.-C., Suh, H.-W., Huh, S.-O., Paek, S.-H., Kim, Y.-H., Kim, S.-H., and Suh, Y.-H. (1998) *J. Neurochem.* **71,** 875–878
30. O'Callaghan, J. P., and Jensen, K. F. (1992) *Neurotoxicology* **13,** 113–122
31. Akiyama, H., Barger, S., Barnum, S., Bradt, B., Bauer, J., Cole, G. M., Cooper, N. R., Eikelenboom, P., Emmerling, M., Fiebich, B. L., Finch, C. E., Frautschy, S., Griffin, W. S. T., Hampel, H., Hull, M., Landreth, G., Lue, L.-F., Mrak, R., Mackenzie, I. R., O'Banion, M. K., Pachter, J., Pasinetti, G., Plata-Salaman, C., Rogers, J., Rydel, R., Shen, Y., Streit, W., Strohmeyer, R., Tooyoma, I., Van Muiswinkel, F. L., Veerhuis, R., Walker, D., Webster, S., Wegrzyniak, B., Wenk, G., and Wyss-Coray, A. (2000) *Neurobiol. Aging* **21,** 383–421
32. Dickson, D. W., Farlo, J., Davies, P., Crystal, H., Fuld, P., and Yen, S. H. (1988) *Am. J. Pathol.* **132,** 86–101
33. Mandybur, T. I., and Chuirazzi, C. C. (1990) *Neurology* **40,** 635–639
34. Matsuoka, Y., Picciano, M., Malester, B., LaFrancois, J., Zehr, C., Daeschner, J. M., Olschowka, J. A., Fonseca, M. I., O'Banion, M. K., Tenner, A. J., Lemere, C. A., and Duff, K. (2001) *Am. J. Pathol.* **158,** 1345–1354
35. Shi, G.-P., Villadangos, J. A., Dranoff, G., Small, C., Gu, L., Haley, K. J., Riese, R., Ploegh, H. L., and Chapman, H. A. (1999) *Immunity* **10,** 197–206
36. Petanceska, S., Canoll, P., and Devi, L. A. (1996) *J. Biol. Chem.* **271,** 4403–4409